

A computational principle trades-off inference and adaptation dynamics

Oded Wertheimer (oded.wertheimer@mail.huji.ac.il)

Edmond and Lily Safra Center for Brain Science, The Hebrew University of Jerusalem
Jerusalem, Israel

Yuval Hart (yuval.hart@mail.huji.ac.il)

Department of Psychology, The Hebrew University of Jerusalem
Jerusalem, Israel

Abstract

The dynamic range of a sensory system reflects the signal levels for which the system is responsive. We propose that dynamic range trades-off between inference (e.g. accuracy, encoding capacity) and dynamic features (e.g. adaptation and updating rates) of the neural computation. We take Autism Spectrum Disorder (ASD), which displays distinct neural and behavioral characteristics compared to the neurotypical (NT) population and show how known results, such as slower environmental adaptability, altered decision-making processes, and altered sensory encoding can be explained by the computational principle of increased dynamic range.

Keywords: Computational principle; Trade-off; neural encoding; autism

Introduction

In recent years, research has mapped many differences between people diagnosed with Autism Spectrum Disorder (ASD) and the neurotypical (NT) population. These differences are reflected in adaptation to changes in the environment (Vishne et al., 2021; Lieder et al., 2019), decision making (Robertson, Martin, Baker, & Baron-Cohen, 2012; Van der Hallen, Manning, Evers, & Wagemans, 2019) and neural encoding (Noel, Zhang, Stocker, & Angelaki, 2021) to name a few. Despite great advances in mapping the myriad of behavioral and neuronal differences, the underlying computational principle that drives them is yet unclear.

A main goal of autism research is finding the driver for the differences in ASD neural activity and behavior. To this end, several computational models have been suggested (Sinha et al., 2014; Van de Cruys et al., 2014; Pellicano & Burr, 2012; Lawson, Rees, & Friston, 2014; Lieder et al., 2019; Rubenstein & Merzenich, 2003; Rosenberg, Patterson, & Angelaki, 2015), and while they provide insights into different behavioral and neural markers that may be linked to ASD, a concrete unifying computational principle that explains the wide range of atypical behaviors and neural activity associated with ASD remains elusive. In this work, we suggest that differences between ASD and NT stem from a simple computational principle manifested in the dynamic range of the neuronal populations when encoding signals. Specifically, we hypothesize that ASD have an increased dynamic range (IDR) compared with NT with a narrow dynamic range (NDR). This computational principle trades-off inference (e.g. accuracy, encoding capac-

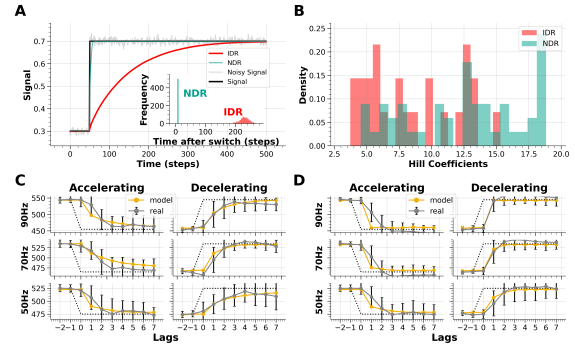


Figure 1: **An increased dynamic range entails slower updating in response to abrupt changes.** (A) A single simulation of tracking an abrupt change in the mean of a noisy signal. Black line - mean signal, Grey line - noisy samples. The noisy signal was encoded by two different populations - gradual population response (Red, $n = 7$) and sharp population response (Turquoise, $n = 16$), and then estimated using Kalman filter. (A, Inset) A histogram of response times to the abrupt change. (B) Histogram of the Hill-coefficients fitted to each individual participant data (Vishne et al., 2021) (C, D) Data and Model fit to ASD (panel C) and NT (panel D) on the group tracking dynamics from Ref (Vishne et al., 2021)

ity) and dynamic features (e.g. adaptation and updating rates) of the neural computation, and explains some phenomena observed in individuals diagnosed with ASD.

Results

Model formulation Dynamic range is the range of input signal values in which the sensing system is responsive. The larger the dynamic range is, the more gradually the system changes from no response to full response. We use the sigmoidal Hill-equation (Hill, 1910) to model the averaged neuronal population response:

$$A_{pop}(S) = \frac{S^n}{S^n + K_m^n} \quad (1)$$

Where $A_{pop}(S)$ is the averaged population neural gain (response) to an input signal S , n is the Hill coefficient, and K_m is the half-activation point of the response function (where the response function reaches half of its maximum value).

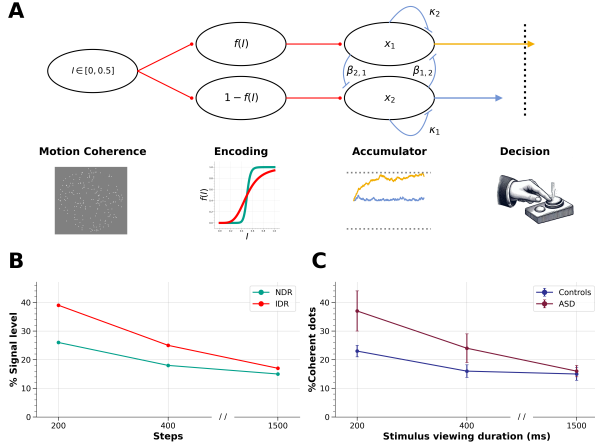


Figure 2: **Increased dynamic range induces elevated detection thresholds in decision making for short integration times.** (A) Illustration of the Leaky Competing Accumulator (LCA) model used to simulate the decision-making process (Usher & McClelland, 2001). (B) The LCA model signal detection levels that elicit 80% correct responses for a narrow dynamic range (NDR, sharp response) and an increased dynamic range (IDR, gradual response) encoders at different maximal simulated decision times. (C) Adaptation of Fig. 3 from a motion coherence task experiment by Robertson et al. (2012).

An increased dynamic range entails slower updating rates to abrupt changes Individuals diagnosed with ASD show slower updating rates to changes in the environment in auditory and motor tasks (Lieder et al., 2019; Vishne et al., 2021). Using Kalman filter for tracking, we estimated the mean input signal from encoded responses to a noisy time-series with an abrupt change. We found that a gradual neuronal population response (IDR) shows slower updating of the estimated signal level. To test the model's predictions, we compared it to the change dynamics from Vishne et al. (2021) experiment (Vishne et al., 2021) (Fig. 1C, D respectively). Consistent with our model predictions, on the individual level the fitted curves result in lower Hill coefficients for the ASD group (mean \pm ste, ASD: 8.5 ± 0.2 , NT: 13 ± 0.1 , Mann-Whitney test $U = 852, p < 10^{-3}$). Similarly, on the averaged group level we fitted the model to the averaged response curve of all participants for each change in tempo (Fig. 1D). We find lower Hill coefficients for the ASD group (mean \pm ste, $n_{ASD} = 7.4 \pm 0.1$ and $n_{NT} = 14 \pm 0.1$, permutation test, $p < 10^{-3}$).

An increased dynamic range increases the detection thresholds for accurate decision making The Motion Coherence Task (Van der Hallen et al., 2019) where participants need to integrate moving dots velocity to decide on a global direction also shows ASD to NT differences in the detection thresholds. A study by Robertson et al. (2012) probed the effect of integration time on the detection thresholds and found

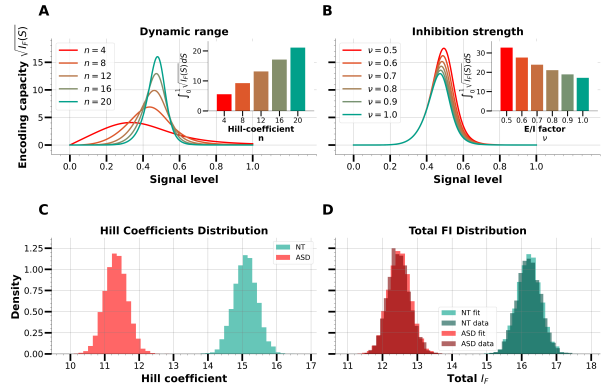


Figure 3: **IDR changes the encoding scheme and reduces the total encoding capacity.** (A) Encoding capacity curves for response function with different Hill-coefficient values, n . (A, Inset) Total encoding capacity. (B) An increased excitation-inhibition ratio model predicts an increase in the encoding capacity as inhibition is decreased. (B, Inset) Total encoding capacity as a function of the inhibitory strength. (C) Fitted Hill coefficients to the "without feedback" block in Noel et al. 2021 for the ASD (Red) and NT (Turquoise) participants (D) Distributions of total encoding capacities for the ASD and NT participants from Noel et al. 2021.

increased thresholds for ASD for short stimulus durations, and comparable thresholds when stimulus viewing durations were long enough (Fig. 2C). To test the performance of the increased dynamic range (IDR) model in this task, we used a known neural model of 2AFC decision making - the Leaky, Competing Accumulator (LCA) model (Usher & McClelland, 2001), which we simulated with an increased dynamic range (IDR, gradual response) and a narrow dynamic range (NDR, sharp response) encoding functions ($n_{IDR} = 8, n_{NDR} = 16$, Fig. 2A, second step, Red & Turquoise lines, correspondingly). Our simulations replicated the results of Robertson et al. (Robertson et al., 2012) by changing only the slope of the encoding function (the Hill-coefficient) highlighting its critical role.

An increased dynamic range alters the encoding scheme We considered the population response to a each signal level as the mean firing rate of a Poissonian neuron and derive a closed-form encoding capacity equation for the population response: $I_F(S) = \frac{n^2 K_m^{2n} S^{n-2}}{(S^n + K_m^n)^3}$. The total encoding capacity ($\int_0^1 I_F(S) dS$) increases linearly with the Hill-coefficient n of the mean firing rate function (see Fig. 3A, Inset) We also fit the increased dynamic range model to the data presented by Noel et al. (2021) and find that fitted Hill-coefficients are lower for the ASD group's data (Fig. 3C-D).

Discussion

We proposed that a simple computational principle, increased dynamic range of the neuronal population response, accounts

for neuronal and behavioral differences between ASD and NT. The dynamic range of the encoding function presents a computational tradeoff between accurate encoding and fast response to an abrupt change in the input signal. On a broader scale, the increased dynamic range model opens new avenues of investigation of the slope of encoding functions as a general principle of neural computation.

tations impedes synchronization in autism. *Nature communications*, 12(1), 5439.

References

- Hill, A. V. (1910). The possible effects of the aggregation of the molecules of haemoglobin on its dissociation curves. *J. physiol.*, 40, 4–7.
- Lawson, R. P., Rees, G., & Friston, K. J. (2014). An aberrant precision account of autism. *Frontiers in human neuroscience*, 8, 302.
- Lieder, I., Adam, V., Frenkel, O., Jaffe-Dax, S., Sahani, M., & Ahissar, M. (2019). Perceptual bias reveals slow-updating in autism and fast-forgetting in dyslexia. *Nature neuroscience*, 22(2), 256–264.
- Noel, J.-P., Zhang, L.-Q., Stocker, A. A., & Angelaki, D. E. (2021). Individuals with autism spectrum disorder have altered visual encoding capacity. *PLoS biology*, 19(5), e3001215.
- Pellicano, E., & Burr, D. (2012). When the world becomes 'too real': a bayesian explanation of autistic perception. *Trends in cognitive sciences*, 16(10), 504–510.
- Robertson, C. E., Martin, A., Baker, C. I., & Baron-Cohen, S. (2012). Atypical Integration of Motion Signals in Autism Spectrum Conditions. *PLoS ONE*, 7(11), 1–9. doi: 10.1371/journal.pone.0048173
- Rosenberg, A., Patterson, J. S., & Angelaki, D. E. (2015). A computational perspective on autism. *Proceedings of the National Academy of Sciences of the United States of America*, 112(30), 9158–9165. doi: 10.1073/pnas.1510583112
- Rubenstein, J., & Merzenich, M. M. (2003). Model of autism: increased ratio of excitation/inhibition in key neural systems. *Genes, Brain and Behavior*, 2(5), 255–267.
- Sinha, P., Kjølgaard, M. M., Gandhi, T. K., Tsourides, K., Cardinaux, A. L., Pantazis, D., . . . Held, R. M. (2014). Autism as a disorder of prediction. *Proceedings of the National Academy of Sciences*, 111(42), 15220–15225.
- Usher, M., & McClelland, J. L. (2001). The time course of perceptual choice: the leaky, competing accumulator model. *Psychological review*, 108(3), 550.
- Van de Cruys, S., Evers, K., Van der Hallen, R., Van Eylen, L., Boets, B., de Wit, L., & Wagemans, J. (2014). Precise minds in uncertain worlds: predictive coding in autism. *Psychological review*, 121(4), 649.
- Van der Hallen, R., Manning, C., Evers, K., & Wagemans, J. (2019). Global motion perception in autism spectrum disorder: a meta-analysis. *Journal of autism and developmental disorders*, 49, 4901–4918.
- Vishne, G., Jacoby, N., Malinovitch, T., Epstein, T., Frenkel, O., & Ahissar, M. (2021). Slow update of internal represen-